Geografiska Annaler: Series A, Physical Geography

ISSN: 0435-3676 (Print) 1468-0459 (Online) Journal homepage: http://www.tandfonline.com/loi/tgaa20

Implications from chemical, structural and mineralogical studies of magnetic microspherules from around the lower younger dryas boundary (new mexico, usa)

Alexandre V. Andronikov, Irina E. Andronikova, Clayton W. Loehn, Barbara Lafuente, Jesse A. M. Ballenger, George T. Crawford & Dante S. Lauretta

To cite this article: Alexandre V. Andronikov, Irina E. Andronikova, Clayton W. Loehn, Barbara Lafuente, Jesse A. M. Ballenger, George T. Crawford & Dante S. Lauretta (2016) Implications from chemical, structural and mineralogical studies of magnetic microspherules from around the lower younger dryas boundary (new mexico, usa), Geografiska Annaler: Series A, Physical Geography, 98:1, 39-59, DOI: 10.1111/geoa.12122

To link to this article: https://doi.org/10.1111/geoa.12122

Published online: 15 Nov 2016.

IMPLICATIONS FROM CHEMICAL, STRUCTURAL AND MINERALOGICAL STUDIES OF MAGNETIC MICROSPHERULES FROM AROUND THE LOWER YOUNGER DRYAS BOUNDARY (NEW MEXICO, USA)

ALEXANDRE V. ANDRONIKOV[1,2], IRINA E. ANDRONIKOVA[2], CLAYTON W. LOEHN[1,5], BARBARA LAFUENTE[1], JESSE A. M. BALLENGER[3], GEORGE T. CRAWFORD[4] and DANTE S. LAURETTA[2]

[1]Department of Geosciences, University of Arizona, Tucson, AZ, USA
[2]Lunar and Planetary Laboratory, University of Arizona, Tucson, AZ, USA
[3]Statistical Research Inc., Tucson, AZ, USA
[4]Eastern New Mexico University, Portales, NM, USA
[5]Shared Instrumentation Facility, Louisiana State University, Baton Rouge, LA, USA

Andronikov, A.V., Andronikova, I.E., Loehn, C.W., Lafuente, B., Ballenger, J.A.M., Crawford, G.T. and Lauretta, D.S., 2016. Implications from chemical, structural and mineralogical studies of magnetic microspherules from around the lower Younger Dryas boundary (New Mexico, USA). *Geografiska Annaler: Series A, Physical Geography*, 98, 39–59. DOI:10.1111/geoa.12122

ABSTRACT. Hollow magnetic microspherules from along the lower Younger Dryas boundary (*c*. 12.9 ka BP) in New Mexico (USA) were studied using scanning electron microscopy, electron probe microanalysis, X-ray diffraction, and laser-ablation inductively coupled-plasma mass spectrometry methods. The shell of the microspherules (10–15% of the spherule's diameter) displays dendritic surface textures, which are likely due to quenching during rapid cooling of molten material. Structurally, multiple single-magnetite crystals attached together form the bulk of the microspherules. Iron dominates the microspherules' composition (~90% FeO_{tot}), Mn is the second most abundant element (up to 0.4% MnO), Al is detected in low concentrations (<0.30% of Al_2O_3). Among the trace elements, the rare earth elements display slightly fractionated patterns with concentrations of 0.1–1.0× CI chondrite. The microspherules contain elevated concentrations of Ni relative to detrital magnetite (up to 435 ppm) and very low concentrations of Ti (down to 5 ppm). Chemical, structural and mineralogical features of the microspherules do not contradict the existing models of the formation during ablation while a meteoroid goes through the Earth's atmosphere. Elevated concentrations of the magnetic microspherules in sediments can be a stratigraphic marker for the lower Younger Dryas boundary in North America.

Key words: magnetic microspherules, trace elements, Younger Dryas

Introduction

The cold period known as the *Younger Dryas* (*YD*) climate oscillation occurred between *c*. 12.9 ka BP and *c*. 11.7 ka BP (e.g. Berger 1990; Peteet 1995; Björck 2007; Lowe *et al.* 2008). This sudden climate change is generally thought to result from an abrupt change of atmospheric and oceanic circulations (e.g. Teller *et al.* 2002; McManus *et al.* 2004; Brauer *et al.* 2008). The beginning of the YD in North America can at times be stratigraphically marked by the so-called black mat, a thin dark layer of organic-rich material (e.g. Firestone *et al.* 2007; Haynes 2007, 2008; Pigati *et al.* 2009, 2012). The black mat, however, is a general term that includes, in addition to the dark organic-rich deposits, some marls and diatomites that are light grey in color (e.g. Ballenger *et al.* 2011). A lot of attention was lately paid to the black mat because of a widespread discussion on the possibility of the extraterrestrial impact shortly before the onset of the YD climate oscillation (e.g. Firestone *et al.* 2007; Haynes *et al.* 2010; Pigati *et al.* 2009, 2012; Andronikov *et al.* 2011, 2014; Fayek *et al.* 2012; Kennett *et al.* 2015). There are reports about findings of unusual objects such as carbon spherules, nanodiamonds, glass-like carbon, melt-glass, as well as enhanced amounts of platinum group elements in sediments corresponding to the *lower YD boundary* (*LYDB*) in support of the hypothesis (e.g. Firestone *et al.* 2007; Kennett *et al.* 2009; Mahaney *et al.* 2010, 2013; Bunch *et al.* 2012; Petaev *et al.* 2013; Wu *et al.*

DOI:10.1111/geoa.12122

2013). One such characteristic object reported is magnetic microspherules (e.g. Firestone *et al.* 2007; Israde-Alcántara *et al.* 2012; LeCompte *et al.* 2012; Wittke *et al.* 2013).

Overall, the magnetic microspherules are tiny (10–250 μm) glossy spherical objects, which are present in variable numbers in Ordovician to Quaternary sediments and sedimentary rocks from multiple sites worldwide (e.g. Blanchard *et al.* 1980; Brownlee *et al.* 1984; Szöőr *et al.* 2001; Gál-Sólymos and Don 2004; Stankowski *et al.* 2006; Franzen and Cropp 2007; van Ginneken *et al.* 2010; Misawa *et al.* 2010; Voldman *et al.* 2012; Bignami *et al.* 2014). The microspherules, often perfectly round in shape, are distinctive among other grains of the host material, indicating that spherule origin is different from that of the rest of sedimentary material. Previously reported LYDB magnetic spherules may deviate from perfectly spherical shape (~10% of spherules) and exhibit teardrop and ovoid shapes with surfaces displaying what appear to be aerodynamic flow features (LeCompte *et al.* 2012; Wittke *et al.* 2013). So far, there are only a few reports on major element composition of the microspherules [sometimes accompanied by *scanning electron microscopy* (*SEM*) observations], and their origin is not clearly established yet (Firestone *et al.* 2007, 2010; Israde-Alcántara *et al.* 2012; Bunch *et al.* 2012; LeCompte *et al.* 2012; Mahaney *et al.* 2013; Wittke *et al.* 2013; Wu *et al.* 2013).

One of the places where a black mat is represented by its light-grey variety and where magnetic microspherules occur is the *Blackwater Draw Locality One* (*BWD-1*) in New Mexico (Fig. 1). The main purpose of the present study is to analyze chemical, structural and mineralogical characteristics of the magnetic microspherules collected from one of the stratigraphic sections of the BWD-1 site (Fig. 2) for better understanding of their origin. We present the results of SEM, *electron probe microanalysis* (*EPMA*), *X-ray diffraction* (*XRD*), and the first-ever results of *laser-ablation inductively coupled-plasma mass spectrometry* (*LA-ICP-MS*) of the magnetic microspherules from the BWD-1 site.

The sedimentary sequence of Blackwater Draw Locality One

The BWD-1 site is located in eastern New Mexico, about 10 km north of the town of Portales and 22 km southwest of the town of Clovis (Fig. 1). Evans (1951) established the classic stratigraphic column for this site. The sediments in this locale are thoroughly dated and a stratigraphic sequence is well established (e.g. Hester 1972; Holliday 1985, 1997; Haynes 1995). The lowest strata are represented by reddish-brown gravel and sand deposits of Late Pliocene to Early Pleistocene age. These lake/pond deposits rest upon bedrock strata separated by a disconformity. The lowest lake/pond deposits are the Gray sand and the Brown sand (Sellards 1952). The Brown sand layer is overlain by the Diatomaceous earth layer (Sellards 1952) separated by a disconformity (so-called "Clovis surface"; Haynes 1995). These basic strata cover the time span from the latest Pleistocene to the latest Holocene, and rest upon Eocene to earlier Pleistocene sands, gravels, and caliche beds.

We sampled the following main units of the sedimentary sequence from the BWD-1 site (after Katz 1997) in order to recover magnetic microspherules (Fig. 2):

- Unit B. Gray sand; from 11 810±90 to 11 380±150 ^{14}C years BP;
- Unit C. Brown sand; 11 290±240 ^{14}C years BP;
- Unit D. Diatomaceous earth; from 10 260±230 to 10 210±110 ^{14}C years BP.

Sample preparation and analytical techniques

Because the sizes of most reported microspherules from the LYDB are <150 μm (Firestone *et al.* 2010; LeCompte *et al.* 2012), the samples of host sediments (~200 g each) were sieved through standard 38, 53 and 125 μm mesh sizes. The magnetic fraction from each sample was separated manually using a grade-52 Nd magnet, and then weighed. The magnetic fractions of <38 μm, 38–53 μm and 53–125 μm were visually inspected under a binocular microscope for the presence of the microspherules. Most magnetic microspherules were found in the 38–53 μm fraction with only a few microspherules in the 53–125 μm fraction. Magnetic microspherules were handpicked from the rest of the magnetic fraction and counted. Sometimes, rounded detrital magnetite and ilmenite grains are almost impossible to distinguish visually from true-marker microspherules, and some rounded magnetite and ilmenite crystals were picked up along with the true microspherules (see the "Results" section).

In order to have clearer images of the structural features of the analyzed material than those available from an optical microscope, we conducted SEM observations. We used a Hitachi S3400N tungsten-filament SEM available at the Arizona LaserChron center housed in the Department of Geosciences of the University of Arizona. Imaging was performed in variable-pressure mode (that

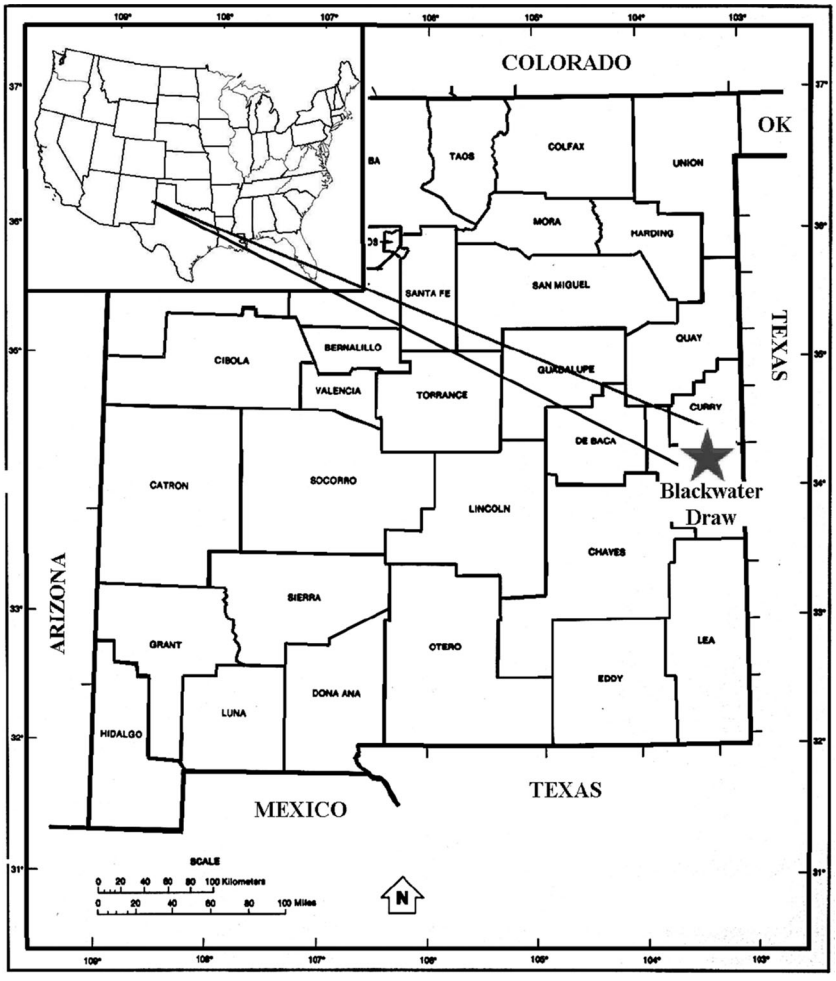

Fig. 1. A map showing the location of the Blackwater Draw Locality One site (BWD-1) in New Mexico, USA (a dark star). The location of the site in the USA is shown as an insert. Source: (modified from www.lib.utex.edu/maps/state/new-mexico.gif)

allows for observations without the need to carbon coat samples) with a beam current of 40–50 pA, an accelerating voltage of 12–20 kV, and a working distance of 7–16 mm. *Energy-dispersive X-ray spectra* (*EDS*) of the microspherules were visually controlled.

We conducted an XRD study with the use of a Bruker X8 Apex single crystal diffractometer equipped with a 4K Apex II CCD detector housed in the Department of Geoscience of the University of Arizona for mineralogical features of the magnetic microspherules. The graphite-monochromatized MoK_α radiation generated at 50 kV and 35 mA, with frame widths 0.5º in ω-scan mode and 30 s counting time per frame was applied.

Magnetic microspherules were analyzed for major oxides with the Cameca SX-50 EPMA at the Lunar and Planetary Laboratory of the University of Arizona. We used an accelerating voltage of 15 kV and current of 20 nA during the analytical runs. The standards used for EPMA calibration are fayalite for Fe, nickel metal for Ni, barite for S, diopside for Ca and Si, apatite for P, cobalt metal for Co, spinel for Cr, Al and Mg, orthoclase for K, vanadium metal for V, rhodochrosite for Mn, rutile for Ti, and zinc metal for Zn.

Concentrations of trace elements in individual microspherules were analyzed with a CETAC Nd:YAG LSX-213 laser coupled with a Thermo Finnigan Element2 ICP-MS at the Lunar and

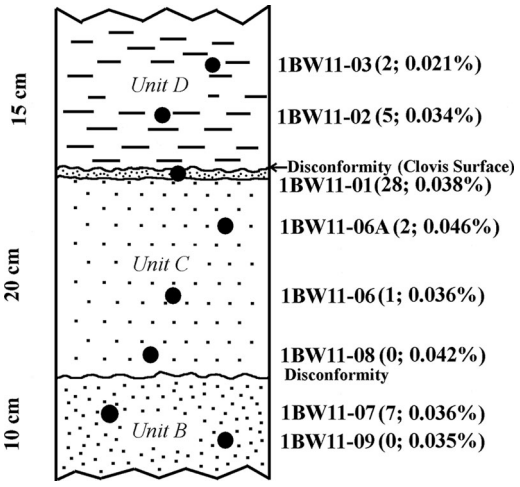

Fig. 2. A stratigraphic column of the studied part of the outcrop 1BW11 of the BWD-1 sedimentary sequence showing the location of the collected samples. A thin (~2 cm) sandy layer at the very top of Unit C (sample 1BW11-01) contains an elevated concentration of magnetic microspherules (numbers of found microspherules and the weight percentage of the magnetic fraction in each sample are given in brackets). This layer is separated from the overlain Unit D by a disconformity known as "Clovis Surface" (Haynes 1995) or the LYDB. Source: (compiled with the use of Sellards 1952 and Haynes 1995)

Planetary Laboratory of the University of Arizona. The applied laser beam diameter was 25 μm, the laser was operated at an energy level 25% of maximum to prevent a fast burn-through of the microspherules. The laser was fired at 20 Hz frequency, for a total of 300 laser shots per sample. The He flow rate was ~700 mL min^{-1}, and the Ar flow rate was ~1.2 L min^{-1}. A NIST SRM 612 silicate glass (Jochum *et al.* 2011) was used as a reference material for the analyzed elements. Repeated analyses of the standards ensured that all results were consistent and comparable. The measurements were based on integrated multi-element time-resolved signals.

Results

While the magnetic fraction varies between 0.02 and 0.05 wt% of each individual sample, there is no systematic pattern in a distribution of the magnetic fraction across the studied part of the sedimentary sequence (Fig. 2). Magnetic microspherules are found in the magnetic fraction in six out of the eight collected samples. Two samples (1BW11-08 of Unit C and 1BW11-09 of Unit B) did not contain any microspherules, the remaining stratigraphic units contain only a very small number of microspherules, and only one sample (1BW11-01 from a thin sandy layer just below the LYDB or "Clovis Surface"; Fig. 2) contains a sufficient number of the microspherules to be used for analytical work. Such distribution of magnetic microspherules across the sedimentary sequence of the BWD-1 site is consistent with the observations made by Firestone *et al.* (2007, 2010) and LeCompte *et al.* (2012). Only six hollow microspherules and two solid microspherule-like objects from the sample 1BW11-01 were large enough to study. A few detrital magnetite and ilmenite grains from the same sample were analyzed as references.

SEM results

The majority of the microspherules are hollow and contain a cavity surrounded by a solid shell that is ~10–15% of a microspherule's diameter. Microspherule surfaces are dendritic, "cob-like" and/or filigreed with a well pronounced orientation of crystals (Fig. 3a, b, d). In one case, a microspherule displays a teardrop-like shape (Fig. 3c). Tiny detrital magnetite grains can be attached to the surface of the microspherules by magnetic forces (Fig. 3e). Sometimes, the outer shell of the microspherules is broken or has an opening (Fig. 3a, f), and the structures of the inner surface can be observed (Fig. 3g, h). The inner structures are either dendritic (Fig. 3g) or polygonal with dendrites present in places (Fig. 3h). On an EDS elemental spectrum, Fe is the dominant element in the composition of the microspherules.

Two of the analyzed microspherules have an appearance that is distinct from the rest of the studied samples (Fig. 3i, j). They are solid and have smooth, slightly corroded surfaces, and spherical to roughly toroidal shapes. These features indicate an origin that is distinct from that of the hollow magnetic microspherules. On an EDS elemental spectrum, Fe and Ti (in approximately equal amounts) are the dominant elements in the composition of the solid microspherules.

XRD results

The single crystal XRD analyses were performed on three hollow microspherules and two solid microspherules already studied with SEM (Fig. 3). The number of diffraction peaks and their locations indicate that the hollow microspheres are formed from multiple randomly oriented single-crystal domains with cubic unit cells that correspond to magnetite with the following

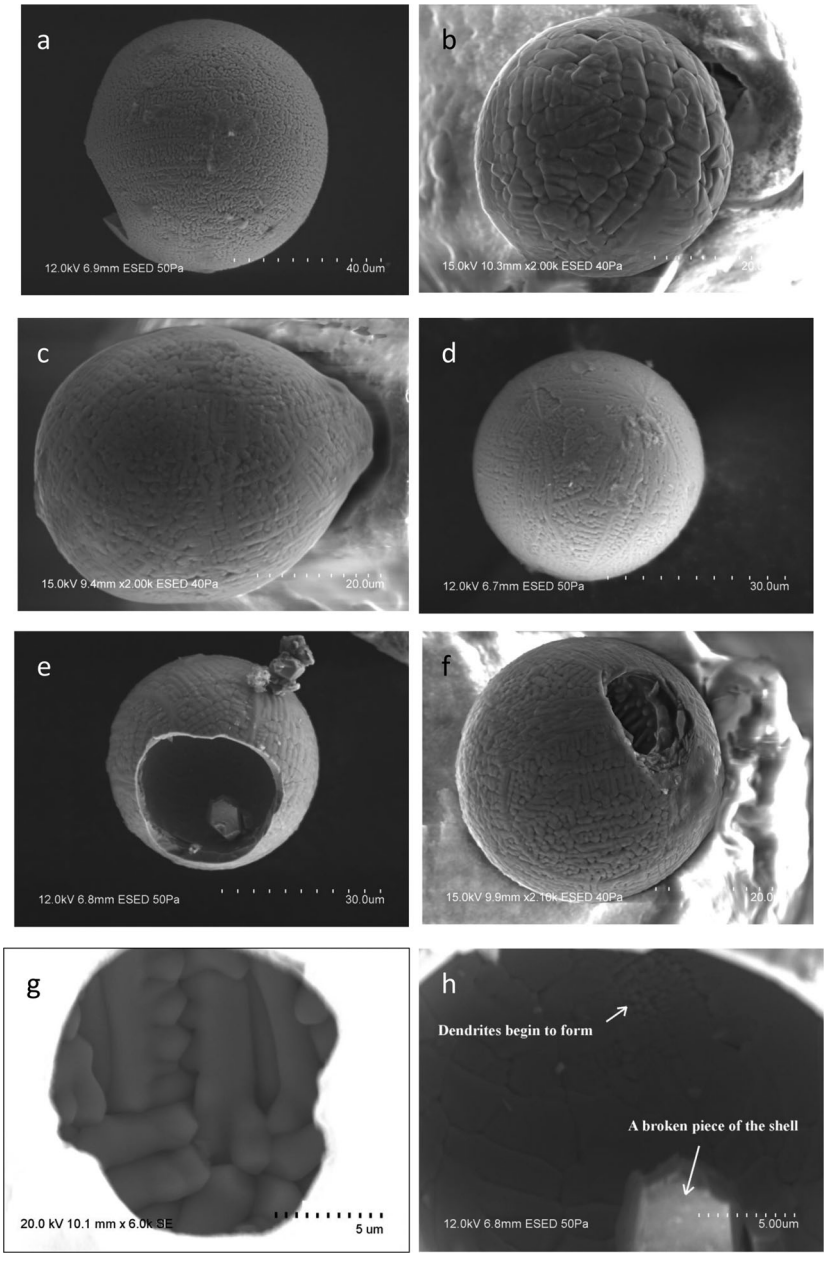

Fig. 3. SEM images of magnetic microspherules from the BWD-1 site: (a) a microspherule displaying dendritic surface structure (the image was taken at an accelerating voltage of 12 kV and a working distance of 6.9 mm); (b) a microspherule displaying a cob-like surface structure (accelerating voltage 15 kV, working distance 10.3 mm); (c) a teardrop-like microspherule displaying dendritic surface structure (accelerating voltage 15 kV, working distance 9.4 mm); (d) a microspherule displaying filigreed surface structure (accelerating voltage 12 kV, working distance 6.8 mm); (e) a broken microspherule with attached magnetite grains and well pronounced filigreed surface structure (accelerating voltage 12 kV, working distance 6.8 mm); (f) a broken hollow microspherule with a thick shell (accelerating voltage 15 kV, working distance 9.9 mm); (g) a microspherule's inner structure as it is seen through the opening (accelerating voltage 20 kV, working distance 10.1 mm); (h) a microspherule's inner structure as it is seen from the broken outer shell (Fig. 3e) (accelerating voltage 12 kV, working distance 6.8 mm); (i) and (j) solid rounded ilmenite grains with corroded surfaces and toroid-like shape (accelerating voltage 15 kV, working distance 15.7 mm; and accelerating voltage 15 kV, working distance 8.2 mm).

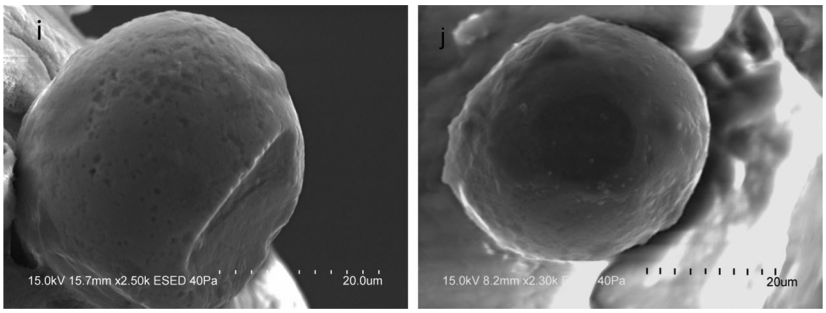

Fig. 3. *Continued.*

parameters: $a = 8.402(6)$ Å and $V = 593.2(4)$ Å^3. The hollow microspherules contain 17–35 single-crystal domains. The unit-cell dimensions, final refined atomic parameters and good reliability factors confirm that the constituent magnetite has a pure Fe_3O_4 composition. Diffraction peaks from other mineral phases were not observed for these three microspherules.

The solid microspherules identified with the SEM both contain one single crystal with a hexagonal unit cell displaying the following parameters: $a = b = 5.065$ Å, $c = 13.92$ Å, and $V = 309$ Å^3. Such cell parameters correspond to minerals from the ilmenite group ($FeTiO_3$). Diffraction spots from other mineral phases were not observed for these two microspherules.

EMPA results

The hollow magnetic microspherules consist mostly of iron oxide (~90% FeO_{tot}). The second most abundant element is Mn (up to 0.4% MnO). Aluminum is usually detected, although in low concentrations (<0.30% of Al_2O_3). Other elements including Ti, Cr, V, Ni, Co, Mg, Ca, Zn, K, P, and S are either present in concentrations close to the detection limits or absent. Only MnO and FeO display slight steady increase in concentrations from the inside parts of the shells toward the outside parts (Table 1). Analytical results show that the microspherules are compositionally distinct from detrital magnetite grains from the same magnetic fraction. In particular, detrital magnetite grains, unlike the microspherules, have high Ti (5.9–20.6% TiO_2) contents (Table 1).

A few analyzed rounded detrital crystals, display compositions corresponding to minerals of the ilmenite group: FeO = 46.1–59.8%, TiO_2 = 37.8–48.7%, MgO = 0.9–5.1%, MnO = 0.5–2.2%, V_2O_3 = 0.20–0.50%. It is notable that such chemical compositions are almost identical to some magnetic microspherules reported by Firestone *et al.* (2010) and LeCompte *et al.* (2012) (Table 2).

LA-ICP-MS results

The analyses showed clear a difference between trace element compositions of the hollow magnetic microspherules and detrital magnetite. None of the hollow magnetic microspherules displays significant amounts of Ti (only 5–460 ppm), whereas the detrital magnetite grains from the same magnetic fraction are Ti rich (16.7–26.2% Ti; Table 3; cf. the EMPA analyses in Table 1). Unlike detrital magnetite, which displays only 1.9–22.8 ppm of Ni, the microspherules are relatively enhanced in Ni with concentrations varying from 148 to 435 ppm. However, magnetite displays much higher concentrations of Zr (91–445 ppm), Nb (14–254 ppm), Hf (4.6–12.2 ppm), Ta (0.9–9.9 ppm), U (0.4–4.4 ppm), and Th (1.3–20.1 ppm) compared with the microspherules (1.3–8.7 ppm, 0.31–23.6 ppm, 0–0.79 ppm, 0.04–0.74 ppm, 0.01–0.22 ppm, and 0.02–0.42 ppm, respectively). Trace-element compositions of rounded ilmenite crystals are distinct significantly from both microspherules and detrital magnetites. Ilmenite displays such features as very high concentrations of Zr (18 030–30 450 ppm), Nb (4500–9500 ppm), Hf (585–655 ppm), Ta (300–385 ppm), Th (37–58 ppm), and U (40–50 ppm), and low concentrations of Cr (42–80 ppm).

All analyzed hollow microspherules display chondritic to subchondritic concentrations of the *rare earth elements* (*REEs*) (0.1–1.0× CI chondrite with La rising up to >10× CI chondrite; Fig. 4). One of the microspherules (MMs#3 in Fig. 4) displays very strong enrichment in Pr-Nd and Gd-Tb-Dy. However, all the rest of the REEs for this microspherule display chondritic

Table 1. Results of microprobe analyses of the magnetic microspherules and detrital magnetite from the BWD-1 site (sample 1BW11-01; wt%).

	MMs#A			MMs#B			MMs#C		
	C	C–E	E	C	C–E	E	C	C–E	E
SiO_2	0.13	0.11	0.05	0.13	0.04	0.04	0.12	0.05	0.04
TiO_2		0.02				0.02			
Al_2O_3	0.24	0.22	0.14	0.18	0.07	0.09	0.26	0.07	0.06
Cr_2O_3			0.11		0.04	0.04	0.03		
V_2O_3	0.04					0.03			
Fe_2O_3*	65.02	66.18	66.26	65.37	66.04	66.01	64.96	65.42	65.71
FeO	29.55	29.98	29.72	29.68	29.59	29.61	29.31	29.28	29.37
MnO	0.18	0.25	0.36	0.17	0.28	0.29	0.23	0.31	0.33
NiO	0.04		0.09			0.07			
CoO		0.04	0.04						
MgO									
CaO	0.03			0.02			0.02		
ZnO		0.04	0.03						
K_2O									
P_2O_5									
SO_3		0.02	0.02		0.03	0.02	0.02		
Total	95.23	96.86	96.82	95.55	96.09	96.22	94.95	95.13	95.51

	MMs#D			MMs#E			MMs#F	MMs#G	MMs#H
	C	C–E	E	C	C–E	E	C	C	C
SiO_2	0.13	0.08	0.07	0.08	0.06	0.05		0.04	0.04
TiO_2	0.04				0.02	0.03			
Al_2O_3	0.15	0.20	0.11	0.14	0.13	0.20	0.06	0.07	0.08
Cr_2O_3	0.05	0.06			0.07	0.04	0.04		0.06
V_2O_3									
Fe_2O_3*	64.53	65.20	65.93	66.04	65.91	65.99	66.46	66.66	66.66
FeO	29.31	29.34	29.53	29.31	29.61	29.63	29.55	29.76	29.80
MnO	0.23	0.35	0.37	0.24	0.34	0.39	0.35	0.37	0.37
NiO	0.12				0.04	0.04	0.07	0.03	0.06
CoO								0.05	
MgO							0.03		
CaO									
ZnO	0.16	0.03							
K_2O	0.03								
P_2O_5	0.04								
SO_3	0.05	0.02	0.04	0.02			0.02	0.03	
Total	94.84	95.28	96.05	95.83	96.18	96.37	96.58	97.01	97.07

	Magnetite			
	1	2	3	4
SiO_2	0.08	0.04	0.12	0.09
TiO_2	5.89	13.81	20.63	15.74
Al_2O_3	3.71	2.28	0.95	1.10
Cr_2O_3	0.09	0.16	0.47	0.05
V_2O_3	0.67	0.49	0.60	0.41
Fe_2O_3*	52.56	40.26	27.23	37.20
FeO	34.43	39.60	45.59	41.50
MnO	0.11	0.29	0.14	1.02
NiO			0.03	
CoO				
MgO	1.43	2.71	2.69	1.98
CaO				
ZnO		0.03	0.04	0.12
K_2O				
P_2O_5				
SO_3				
Total	98.97	99.67	98.49	99.21

C, central part of the shell; C–E, between the central and edge parts of the shell; E, the edge part of the shell; MM, hollow magnetic microspherule.
*Fe_2O_3 is calculated from stoichiometry.

Table 2. Chemical composition of rounded ilmenite grains from the BWD-1 site in comparison with high-Ti microspherules (Firestone *et al.* 2010; LeCompte *et al.* 2012) (wt%).

	Ilmenite							
	1	2	3	4	5	6	7	8
SiO_2	0.04	0.10		0.04	0.10	0.04		0.03
TiO_2	48.66	45.33	38.30	39.57	37.76	40.86	44.29	39.23
Al_2O_3	0.19	0.99	0.23	0.30	0.35	0.11	0.49	0.13
Cr_2O_3	0.02	0.03	0.02		0.02			0.04
V_2O_3	0.32	0.43	0.28	0.40	0.31	0.23	0.48	0.21
FeO_{tot}	47.79	46.09	57.41	55.55	59.84	54.37	49.00	57.04
NiO		0.07		0.05	0.07	0.04	0.02	0.02
CoO		0.03			0.03			
MgO	2.46	5.12	2.07	3.04	0.87	1.95	5.10	1.65
MnO	0.62	1.38	1.40	0.66	0.46	2.23	0.53	1.79
CaO		0.00						
ZnO		0.08		0.06	0.02	0.10		0.02
Na_2O		0.02	0.04	0.04		0.02	0.02	
K_2O								
P_2O_5								
SO_3	0.02		0.12	0.02		0.04	0.11	
Total	100.12	99.69	99.87	99.73	99.84	99.99	100.04	100.16

	Firestone *et al.* (2010)			LeCompte *et al.* (2012)				
SiO_2	3.1	4.5	4.6	3.33	2.29	1.68	2.99	4.27
TiO_2	53	47	40	53.89	57.7	32.65	31.95	39.41
Al_2O_3	2.3	2.7	3.0	2.42	1.10	2.19	3.41	2.37
Cr_2O_3				0.01			0.01	0.05
V_2O_3	n.d.	n.d.	n.d.	n.d.	n.d.	n.d.	n.d.	n.d.
FeO_{tot}	37	44	50	37.12	36.49	59.86	55.29	45.22
NiO	n.d.	n.d.	n.d.				0.02	0.01
CoO	n.d.	n.d.	n.d.	n.d.	n.d.	n.d.	n.d.	n.d.
MgO				1.59	0.27	2.69	4.68	6.3
MnO	3.5	1.7		0.26	0.58	0.12	0.07	1.01
CaO				0.13	0.25	0.14	0.38	0.01
ZnO	n.d.	n.d.	n.d.	n.d.	n.d.	n.d.	n.d.	n.d.
Na_2O				1.02	0.43	0.02	0.78	1.33
K_2O				0.03	0.03	0.03		0.02
P_2O_5				0.20	0.26	0.33	0.37	
SO_3					0.60	0.29	0.03	
Total	98.9	99.9	97.6	100.00	100.00	100.00	99.98	100.00

n.d., no data available.

and subchondritic concentrations as is typical for the other microspherules analyzed. In contrast to the hollow microspherules, detrital magnetite grains display smooth REE patterns with elemental concentrations well above the chondritic level (3–500× CI chondrite for different REEs). The magnetite's REE pattern style is often similar to that of the host sediments (Fig. 4). Rounded ilmenite crystals are enriched in heavy (H)REE (up to 240× CI for Lu) and display a strong Eu negative anomaly (Fig. 4) as it is typical for terrestrial ilmenites from elsewhere.

Because of a small laser beam diameter (25 μm), low applied laser energy (25% of maximum) and overall low *platinum group elements* (*PGEs*) concentration in the microspherules, the PGE signal intensities during analytical runs were very low (except for Pd), only slightly above the detection limit. Although the results of the LA-ICP-MS analyses suggest the presence of the PGE in the BWD-1 microspherules (Table 3), the measured concentrations are subject to very high analytical errors and are comparable with the concentrations in detrital magnetite and ilmenite. Therefore, concentrations of the PGE are given for informative purposes only (Table 3).

Discussion

Overall, Fe-rich magnetic microspherules from elsewhere (also known as I-type microspherules; e.g. Franzén 2006; Franzén and Cropp 2007) can be of volcanic, industrial, biogenic and diagenetic, and

cosmic origins. In order to talk about origin of the microspherules, it is necessary to distinguish first between true-marker microspherules and rounded detrital magnetic crystals. Our SEM, XRD, EMPA, and LA-ICP-MS data suggest that some spherical objects looking very similar under the microscope to hollow magnetic microspherules are in reality single-crystal minerals of the ilmenite group (Tables 2 and 3). These data rule out the cosmic origin of such "microspherules".

Another marker pointing to a possible origin of the microspherules is Ti. Because magnetic particles of cosmic origin contain only negligible amounts of Ti (e.g. Szöőr *et al.* 2001; Grachev *et al.* 2008; Voldman *et al.* 2012 and references therein), the element is useful to distinguish between terrestrial and extraterrestrial magnetic particles. For example, volcanic magnetic microspherules (real microspherules, not rounded crystals) are always titaniferous, (usually >10% of Ti) and, as important, are never hollow (Cornen *et al.* 1992; Grebennikov 2011; Voldman *et al.* 2012 and references therein). However, while low concentration of Ti is possible in detrital magnetite crystals of metamorphic and igneous origins (not so low though as in cosmic microspherules), they never occur as real spherules, are never hollow, and never display dendritic surfaces. Therefore, low amounts of Ti accompanied by a hollow shape, and the presence of dendritic surfaces reliably rule out both a volcanic origin and a detrital (initially metamorphic or igneous) origin of the microspherules from the BWD-1 site.

Some spherical magnetic objects from the BWD-1 site reported by Firestone *et al.* (2007, 2010), and LeCompte *et al.* (2012) contain very high Ti abundances (Table 2), whereas our study points to virtually Ti-free composition of the hollow magnetic microspherules studied. Moreover, it is notable that compositions of terrestrial magnetite and ilmenite from the BWD-1 site are very close to the compositions of some microspherules described by Firestone *et al.* (2007, 2010) and LeCompte *et al.* (2012) (Tables 1–3). It is possible, therefore, that Ti-rich magnetic objects analyzed by Firestone *et al.* (2007, 2010) and LeCompte *et al.* (2012) represent microtektites. This would explain their composition, which is uncharacteristic for cosmic microspherules. Thus, the presence of Ti-magnetite spherules can be an indicator of terrestrial impact ejecta. In the present study, however, we did not encounter such Ti-rich microspherules.

Magnetic microspherules of industrial origin are the most difficult to distinguish from the cosmic microspherules (e.g. Vuorelainen and Törnroos 1986; Horng *et al.* 2009; Marini and Raukas 2009; Uscinowicz 2009). However, unlike the cosmic microspherules, the magnetic microspherules of the industrial origin are usually characterized by smooth, polished surfaces (no dendritic structures), and may often have grains of zircon (and other minerals) welded upon them (Marini and Raukas 2009; Uscinowicz 2009; Voldman *et al.* 2012). The BWD-1 microspherules possess characteristic dendritic surfaces (Fig. 3a–f), which are inconsistent with typical industrial origin. Moreover, bulk concentrations of Zr are very low in the studied hollow microspherules (1.3–8.7 ppm), precluding the existence of zircon grains welded upon the microspherules. All this would not overall be sufficient to rule out the origin of the studied hollow microspheruels as industrial, but it is very important that they were found in high numbers only inside a thin layer deposited *c*. 12.9 ka BP (Fig. 2). Therefore, the involvement of modern technological processes in the generation of the hollow magnetic microspherules from the BWD-1 site has been ruled out.

In addition to the processes described above, some terrestrial magnetite can be produced both biogenically under anaerobic conditions and chemically during pedogenic processes involving carbon-rich soils. However, magnetite grains of such origin are extremely small (nanometers) and always display a crystalline shape (Towe and Moench 1981; Vali *et al.* 1987; Stolz *et al.* 1990; Kim *et al.* 2005; Kopp *et al.* 2006; Lippert and Zachos 2007; Schumann *et al.* 2008). It is worth noting that a diagenetic origin has been suggested for magnetic microspherules in several carbon-bearing sediments and in bitumen from mid-Ordovician carbonate rocks of North America (McCabe *et al.* 1987; McWhinnie *et al.* 1990; Saffer and McCabe 1992). However, no evidence in support of such an origin was provided. Moreover, it may be diagnostic that such microspherules were found in sediments of the mid-Ordovician age, strata known worldwide to carry numerous magnetic microspherules related to a sharp increase of meteoritic influx (e.g. Schmitz *et al.* 2008; Dredge *et al.* 2010; Cronholm and Schmitz 2010; Misawa *et al.* 2010; Lindskog *et al.* 2012; Voldman *et al.* 2012). Therefore, the mid-Ordovician microspherules in North America are likely connected with the increased meteoritic flux, and have nothing to do with diagenetic processes. Rare magnetite microspherules in sediments and sedimentary rocks may also originate by alteration

Table 3. Results of the LA-ICP-MS analyses of the magnetic microspherules, and detrital magnetite and ilmenite from the BWD-1 site (normalized to 100%).

	MMs#1	MMs#2	MMs#3	MMs#4	MMs#5	MMs#6
Fe (%)	99.54	99.67	99.60	99.73	99.28	99.54
Ti (ppm)	5.079	196.1	60.56	141.8	324.4	460.0
V	7.871	25.82	42.42	24.25	58.02	48.72
Cr	191.2	167.0	155.6	168.7	360.4	140.3
Mn	1376	1188	1373	571.1	2688	685.1
Co	59.43	40.10	39.30	30.89	123.5	48.13
Ni	255.8	183.4	353.6	147.7	434.6	365.9
Zn	2680	1493	1488	1584	3130	2820
Y	0.321	0.233	0.468	1.308	2.220	0.167
Zr	1.300	2.688	3.984	5.195	8.661	5.049
Nb	0.349	7.206	0.310	7.670	21.87	23.55
La	0.122	3.626	0.650	1.577	1.914	0.102
Ce	0.118	3.976	0.794	0.841	0.927	0.249
Pr	0.046	0.789	83.67	0.155	0.245	0.194
Nd	0.140	3.225	144.9	0.105	0.465	0.578
Sm	0.054	0.244	0.155	0.037	0.120	0.195
Eu	0.048	0.165	0.056	0.028	0.040	0.013
Gd	0.534	0.515	27.02	0.069	1.209	0.180
Tb	0.007	0.025	0.158	0.006	0.044	0.008
Dy	0.017	0.346	6.130	0.052	0.208	0.042
Ho	0.023	0.054	0.024	0.007	0.013	0.006
Er	0.152	0.114	0.090	0.052	0.233	0.013
Tm	0.006	0.098	0.023	0.004	0.029	0.005
Yb	0.132	0.049	0.037	0.138	0.041	0.031
Lu	0.011	0.035	0.004	0.010	0.017	0.005
Hf	bdl	0.046	0.374	0.787	0.146	0.314
Ta	0.041	0.199	0.092	0.335	0.303	0.735
W	0.861	4.821	4.641	3.804	3.563	3.630
Th	0.021	0.055	0.419	0.272	0.326	0.070
U	0.026	0.156	0.219	0.055	0.141	0.007
Ru (ppb)	6.94	47.4	bdl	53.6	10.2	bdl
Rh	95.6	91.2	79.1	12.2	835	111.9
Pd	53.6	49.5	28.2	7.80	134	103
Re	4.70	bdl	5.21	2.78	9.82	bdl
Os	bdl	bdl	bdl	1.11	7.67	3.21
Ir	1.89	bdl	bdl	1.48	5.05	0.410
Pt	80.6	bdl	22.1	18.2	460	bdl
	Mgt-1	Mgt-2	Mgt-3	Mgt-4	Ilm-1	Ilm-2
Fe (%)	73.04	80.63	73.29	81.57	53.54	54.62
Ti	261983	180451	256427	167204	408998	428407
V	1954	3360	3712	2861	1812	3712
Cr	168.6	628.6	809.1	555.8	41.65	80.11
Mn	2499	1682	2737	3937	5357	3257
Co	94.23	135.9	276.5	181.8	130.7	126.5
Ni	1.860	8.402	22.78	20.57	37.49	27.81
Zn	2102	640.3	1110	502.9	246.4	209.7
Y	6.281	12.16	10.2	3.757	89.76	102.0
Zr	444.6	168.6	91.26	312.0	30449	18026
Nb	217.2	13.78	254.4	46.28	9483	4544
La	4.772	6.639	3.200	0.332	0.517	0.320
Ce	4.828	17.64	3.456	1.873	0.460	0.300
Pr	1.057	1.758	2.872	0.231	0.032	0.088
Nd	4.028	6.561	7.803	1.351	0.270	0.218
Sm	0.705	1.032	1.09	0.627	0.188	0.270
Eu	0.152	0.348	0.260	0.079	0.048	0.060
Gd	0.793	0.693	0.832	0.614	2.052	1.432
Tb	0.093	0.081	0.268	0.131	0.572	0.684
Dy	0.503	0.400	1.943	0.833	7.193	9.430

Table 3. Continued

	Mgt-1	Mgt-2	Mgt-3	Mgt-4	Ilm-1	Ilm-2
Ho	0.142	0.164	0.419	0.147	2.522	4.188
Er	0.443	0.512	1.277	0.490	12.73	18.77
Tm	0.091	0.108	0.206	0.051	3.117	2.058
Yb	0.785	1.022	1.672	0.463	34.42	26.72
Lu	0.150	0.166	0.224	0.059	5.874	4.091
Hf	12.19	4.569	7.571	8.577	584.6	657.1
Ta	9.809	0.807	8.756	2.661	385.6	298.0
W	0.509	2.409	13.16	7.782	7.286	10.02
Th	11.51	20.07	15.80	1.274	37.63	57.99
U	1.813	4.435	3.926	0.430	39.72	49.51
Ru	6.52	11.4	bdl	18.7	6.08	7.74
Rh	7.39	6.55	28.3	16.9	3.98	3.30
Pd	29.8	32.1	111	84.6	65.4	21.3
Re	10.4	0.634	4.43	7.43	4.53	3.43
Os	bdl	bdl	bdl	bdl	bdl	bdl
Ir	bdl	bdl	bdl	bdl	bdl	bdl
Pt	27.6	bdl	7.00	bdl	22.0	8.00

bdl, below detection limit; Ilm, ilmenite; Mgt, magnetite; MM, magnetic microspherule.

of framboidal pyrite, but such microspherules display very specific surface structures (Suk *et al.* 1990; Franzén 2006; Bunch *et al.* 2012), which is inconsistent with structure display observed for the hollow microspherules from the BWD-1 site. Therefore, both biogenic and diagenetic origins for the hollow magnetic microspherules from the BWD-1 site can be ruled out.

At the BWD-1 site, common terrestrial forms of hollow magnetic microspherules have been ruled out, but there is no direct evidence for their cosmic origin either. Certain microspherule composition characteristics can shed light on their origin. We plotted concentrations of selected trace elements against Ni (as an indicative element for the meteoritic component) and against Ti (as an indicative element for the terrestrial component) (Figs 5 and 6). Concentrations of Ti in the microspherules mainly correlate positively with concentrations of the elements that are characteristic of terrestrial Ti-magnetite and ilmenite, whereas concentrations of Ni correlate positively with concentrations of the elements – typical constituents of meteorites (e.g. Anders and Grevesse 1989). Elevated concentrations of such "terrestrial" elements as Ta, Nb, and Ti in some hollow microspherules (Table 3) are likely due to contamination by tiny detrital Ti-magnetite grains attached to microspherule surfaces (Fig. 3e). Elevated concentrations of Mn, and its positive correlation with Ni could be an intrinsic feature of the microspherules, putting them in the transition from Fe to Fe-Mn chemical type of microspherules (cf. Gál-Sólymos and Don 2004).

Another group of the elements, REEs, can be used to understand the nature of the microspherules. The REEs are about 300 times more common in terrestrial materials than in meteorites (e.g. Anders and Grevesse 1989; Wedepohl 1995; Franzén and Cropp 2007). The REE composition of the BWD-1 hollow microspherules is distinct from either that of detrital magnetite and ilmenite or of the host sediments (Fig. 4). The light (L)REE are very mobile, and the abundances of such elements can be easily compromised by the post-deposition terrestrial processes whereas *medium REEs* (*MREEs*) and especially heavy REEs (*HREEs*) are much more resistive to post-deposition terrestrial processes, and their concentrations are more likely to correspond to the original compositions. Overall, the MREEs and HREEs in the hollow microspherules studied display mostly chondritic and subchondritic concentrations, whereas concentrations and distributions of the REEs in detrital magnetites and rounded monocrystals of ilmenite are distinctly different (Table 3; Fig. 4). One of the analyzed microspherules (MMs#3) displays a very complex REE pattern characterized by strong enrichments in Pr-Nd and Gd-Tb-Dy (Fig. 4). It is appropriate to suggest that such behavior of the REEs could be either resultant from strong contamination by terrestrial material, or due to the microtektitic origin of the microspherule (cf. LeCompte *et al.* 2012; Wittke *et al.* 2013; Wu

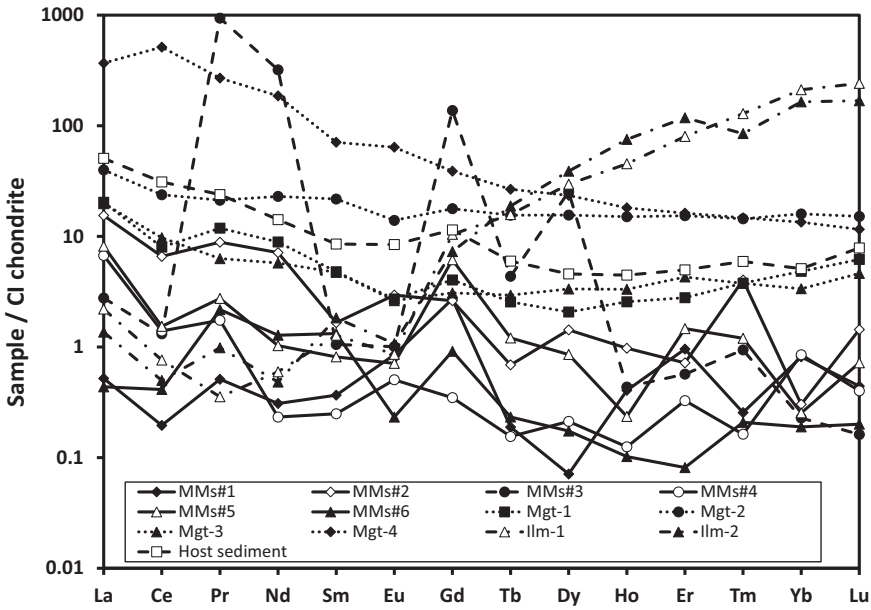

Fig. 4. CI chondrite-normalized diagram for the magnetic microspherules, detrital magnetite and ilmenite from the BWD-1 site. Normalizing values are after Anders and Grevesse (1989). The REE composition of the host sediments is given for comparison (author's unpublished data).

et al. 2013). However, the rest of the REEs in the MMs#3 behave consistently with the REEs from other microspherules. The observed near chondritic REE abundances in the hollow microspherules accompanied by only very slight REE fractionation distinguish them significantly from the analyzed terrestrial material (cf. Rudraswami *et al.* 2012).

Among the trace elements, the PGE and Ni are the most reliable indicators for a cosmic origin (e.g. Sawlowicz 1993; Palme 2008). Metallic micrometeorites and solid cosmic microspherules, which are a part of the constant cosmic influx, usually contain high concentrations of Ni. However, hollow magnetic microspherules from elsewhere either display low concentrations of Ni (up to several per cents) or are virtually Ni free (Bonté *et al.* 1987; Koeberl and Hagen 1989; Bi *et al.* 1993; Marini *et al.* 2004; Stankowski *et al.* 2006; Genge *et al.* 2008; Guaita and Martegani 2008; van Ginneken *et al.* 2010; Rudraswami *et al.* 2014a, 2014b). However, although high Ni content indicates extraterrestrial origin, low concentrations of Ni do not rule out such an origin (e.g. El Goresey and Fechtig 1967; El Goresey 1968; Rochette *et al.* 2009). In the case of Fe oxide-rich microspherules in general, the PGE (when present) are not evenly scattered through the Fe-rich material, but mainly concentrate in nuggets ($\sim$1 μm size; e.g. Rudraswami *et al.* 2014a, 2014b). In the case of the BWD-1 microspherules, the absence of the reliably detectable PGE does not preclude the presence of the PGE nuggets. Since such nuggets are extremely small, their relative contribution to the bulk composition of the microspherules will probably be almost undetectable. Therefore, although there is no unequivocal geochemical evidence of the cosmic origin of the BWD-1 microspherules, their trace element composition does not contradict to such origin either.

Mineralogically, the hollow magnetic microspherules from the BWD-1 site consist of multiple single-magnetite crystals attached to each other whereas studied macroscopically similarly looking rounded ilmenite grains consist of a single ilmenite crystal each. The presence of dendritic textures on surfaces of the hollow microspherules (and sometime a tear drop-like shape of the microspherule; Fig. 3c) is consistent with quenching under rapid cooling of droplets of molten material (e.g. Szöőr *et al.* 2001). The absence of wüstite, a metastable phase typical in micrometeorites and in microspherules resulting from experiments simulating high-altitude ablation (e.g. Blanchard 1972; Brownlee *et al.* 1975),

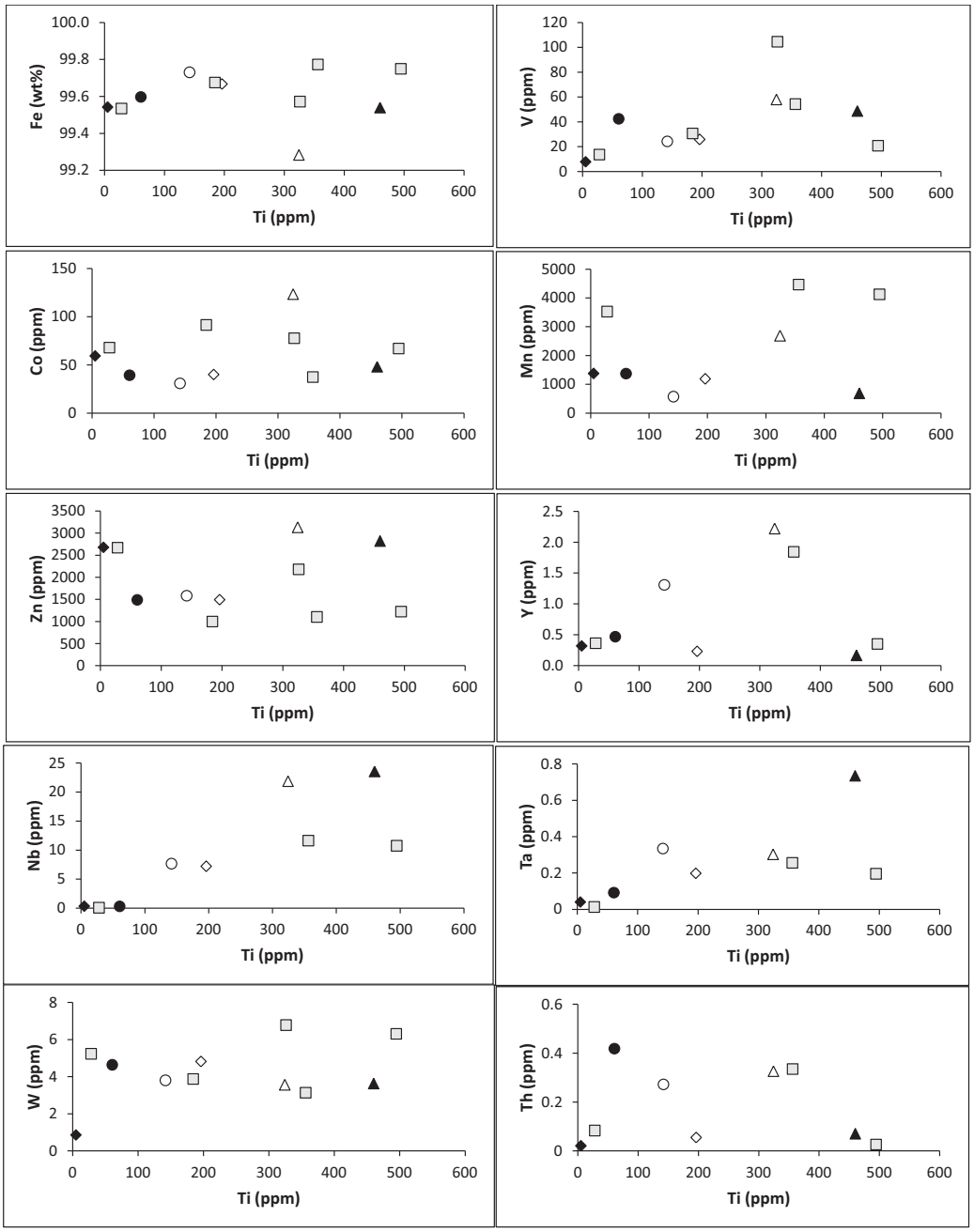

Fig. 5. Binary diagrams Ni vs. selected trace elements for the magnetic microspherules from the BWD-1 site. There are visible correlations between Ni and Fe (negative), Ni and Co (positive), and, to some lesser extent, between Ni and Zn (positive), and between Ni and Mn (positive). Grey squares are microspherules from the LYDB of Murray Springs (AZ) given for comparison (authors' unpublished data). The rest of the legend as in Fig. 4.

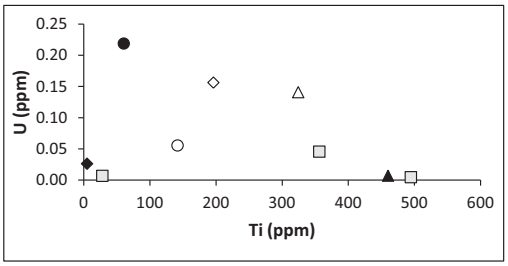

Fig. 5. *Continued.*

precludes the origin of the hollow microspherules from the BWD-1 site as a part of the background cosmic dust population, which melts at high altitudes (mostly above 80 km; Vondrak *et al.* 2008). Instead, the dominance of magnetite is consistent with formation in an environment with a high partial pressure of oxygen (see section below "Possible mechanisms . . . ").

Hollow magnetic microspherules from elsewhere

Hollow magnetic microspherules displaying structures very similar to those observed for the BWD-1 microspherules are known across the temporal sequence from modern sediments to as deep in the past as in the Ordovician (e.g. Iwahashi 1991; Colombetti *et al.* 1998; Franzén 2006; Guaita and Martegani 2008; Dredge *et al.* 2010; Bunch *et al.* 2012; Voldman *et al.* 2012; Tselmovich 2013; Tselmovich *et al.* 2013). The microspherules in some localities are known to be related to meteoritic events. For example, the magnetic microspherules in the Morasko Meteorite Nature Resort (Poland) known to result from the ablation of an iron meteorite (so-called iron-dust shower; Stankowski *et al.* 2006) include some that are very similar to the BWD-1 microspherules by their hollow shapes, dendritic surfaces, absence or low concentration of Ni in Fe oxides, and presence of magnetite lacking wüstite. Microspherules very similar to the BWD-1 hollow microspherules in appearance (dendritic surfaces) and composition (Ni-free magnetite) are reported from near the Kamil meteorite crater in Egypt (Bignami *et al.* 2014). Hollow (although Ni-bearing) magnetic microspherules resulting from ablation of the Sikhote Alin (Russia) iron meteorite, are reported by Badyukov and Raitala (2012). Study of the ablation products of the Chelyabinsk (Russia) stony meteorite showed the presence of hollow microspherules very similar in appearance to those considered in the present work (Tselmovich 2013; Tselmovich *et al.* 2013). Therefore, at least some hollow magnetic microspherules (both Ni-poor/free and Ni-bearing) can be meteorite ablation byproducts. Some microspherules resulted from the increased meteorite flux in the mid-Ordovician (*c*. 470 Ma) display surface structures which are very similar to those observed for the BWD-1 microspherules (e.g. Szőőr *et al.* 2001; Marini *et al.* 2004; Stankowski *et al.* 2006; Guaita and Martegani 2008; Schmitz *et al.* 2008; Dredge *et al.* 2010; Badyukov and Raitala 2012; Voldman *et al.* 2012). Because of the close similarity in chemical, structural, and mineralogical characteristics of the BWD-1 hollow microspherules to those directly related to known meteorite-related events, the cosmic origin (meteorite ablation) seems to be a credible hypothesis for the formation of the BWD-1 hollow magnetic microspherules.

Possible mechanisms for hollow magnetic microspherule formation

Few pulse-heating experiments have been conducted in order to explain atmospheric entry phenomenon (Blanchard 1972; Blanchard and Cunningham 1974; Del Monte *et al.* 1974a, 1974b, 1976; Blanchard and Davis 1978; Fraundorf *et al.* 1982; Sandford and Bradley 1989; Greshake *et al.* 1998; Toppani *et al.* 2001; Guaita and Martegani 2008). Some of these experiments resulted in generation of magnetic microspherules (Blanchard 1972; Del Monte *et al.* 1974a,b, 1976; Blanchard and Davis 1978; Guaita and Martegani 2008). Based on such experiments and on theoretical constraints, we suggest two main models to explain the features displayed by the hollow microspherules from the BWD-1 site.

The first model is based on the experiments simulating the incineration of a meteorite during passage through the Earth's atmosphere. During melting and fast cooling of Fe and Fe-Ni particles in the air flow at varying air pressure, magnetic microspherules of different structural

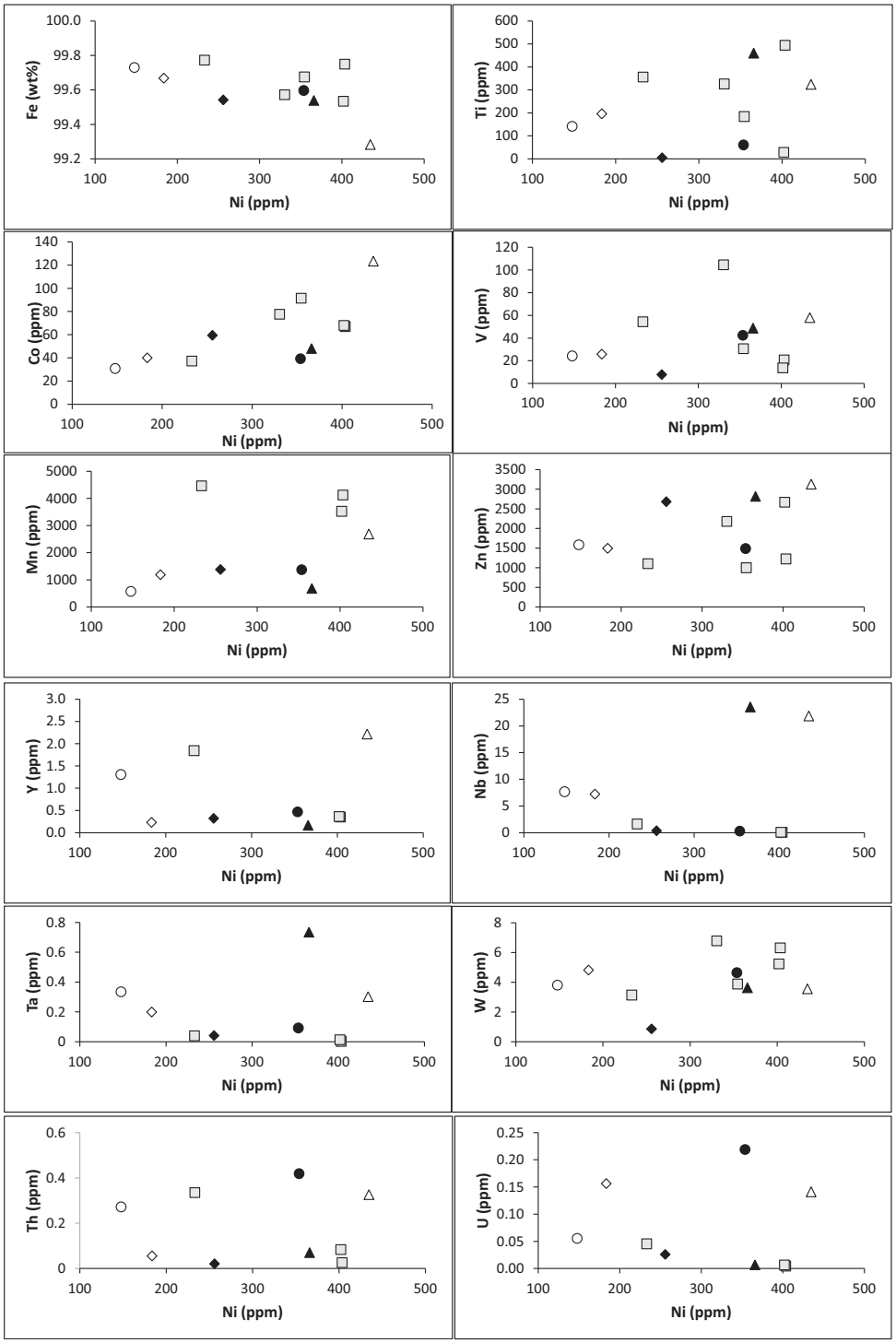

Fig. 6. Binary diagrams Ti vs. selected trace elements for the magnetic microspherules from the BWD-1 site. Ti displays a positive correlation with Ta and Nb, and a lesser pronounced positive correlation with V and Fe. The legend as in Figs 4 and 5.

types were produced (Del Monte *et al.* 1974a, 1974b, 1976). Many of the experiment-generated magnetic microspherules were hollow. It was determined that the presence/absence of a cavity inside the microspherule strongly depended on partial pressure of O_2 in the melt/cool atmosphere stage. A number of the hollow microspherules produced increased with the increase in air pressure. Small numbers of the hollow microspherules initiated at air pressure starting from as low as 30 hPa (corresponds to the altitude of 21.5 km). The number of hollow spherules and size of the cavity increase as the O_2 partial pressure is rising, reaching 90% of the total number of the produced microspherules at air pressures >470 hPa (~6 km). Since the solubility of O_2 in molten Fe is elevated at high temperature (Ohtani and Ringwood 1984), molten iron-rich particles absorb the oxygen molecules they encounter, and quickly oxidize all Fe-rich particles. However, when particles cool, solubility of O_2 decreases and the excess oxygen releases from the liquid in the form of bubbles that move toward the center of the spherule and form cavities. Sometimes, oxygen escapes from the spherules before complete crystallization leaving behind an opening.

The experiments of Blanchard (1972), and Blanchard and Davis (1978) simulated meteor passage and ablation at an altitude of ~70 km (air pressure <1 hPa). During melting of metallurgical iron (99% Fe) and Ni-Fe (10% Ni) alloys, more than 90% of the resultant ablation debris are microspherules of 50–100 μm size. The most abundant resultant spherules contain a Ni-rich core surrounded by an iron oxide shell. No hollow spherules were produced during these ablation experiments as high-altitude conditions were simulated, where the partial pressure of oxygen is too low to form hollow microspherules (see Del Monte *et al.* 1974a, 1974b, 1976). Experiments at both low and high atmospheric pressures showed that magnetic microspherules (not necessarily hollow) easily result from ablation of Fe and Ni-Fe material.

High-temperature heating experiments (up to 1600°C) by Guaita and Martegani (2008) simulated atmospheric entry of stone (ordinary chondrite) and iron (Fe plus 7% Ni) meteorites. The authors showed that the magnetic microspherules can be generated from both material types. In stony meteorites, microspherules showed composition and structures similar to those known for the hollow magnetic microspherules of the I-type (e.g. Franzén and Cropp 2007). In the case of iron meteorites, both Fe-rich and Fe with traces of Ni microspherules morphologically similar to the microspherules of the I-type were produced.

The second suggested model is based on theoretical constraints. Brownlee *et al.* (1984) on the basis of studying various microspherules suggest that Si-rich cosmic material, which melts during atmospheric entry and passage, forms combined spheroids of molten silicate and metal. These two fractions are separated by forces of inertia and form individual metal and silicate spheres. Silicate spheres are beyond the scope of the present study. Metal spheres then differentiate to Fe oxide shells and Ni- and PGE-rich cores (cf. Blanchard 1972; Blanchard and Davis 1978). At the end of complete oxidation, the Ni-rich core eventually leaves the spherule, and finally a small PGE nugget forms. Toppani *et al.* (2001) studied theoretical constraints on the origin of the hollow magnetite microspherules during the pulse-heating experiments simulating the atmospheric entry of micrometeorites and suggested that the most plausible mechanism is a peripheral partial melting during the ablation with subsequent magnetite crystallization.

The third mechanism is proposed by Marini *et al.* (2004) who suggested that in the case of an asteroid (meteorite) fall, the energy released by the impact (airburst) is sufficient not only for melting the material of the falling body but also for its evaporation. Metal vapors could have been raised by the explosion to a height up to tens of kilometers, where their crystallization took place (Grachev *et al.* 2008). Because of the difference in evaporation temperatures (boiling point for Fe is 2750°C, and for Ni is 2732°C, both of which are much lower than boiling points for the PGE), the growth from the vapor phase gives an explanation for the lack of Ni and especially the PGE in the magnetic microspherules of the studied type (cf. Marini *et al.* 2004; Wittke *et al.* 2013). All particles resulting from the impact/airburst bear clear indications of their origin from liquids, and they all bear imprints of similar conditions of surficial cooling. During the surface impact, the molten particles interact with atmospheric O_2 at high pressure that favors generation of hollow spherules as shown by Del Monte *et al.* (1974a, 1974b, 1976). However, during impact, the mixing of the impactor and target materials takes place. Therefore, the impact-related microspherules would carry mixed terrestrial/ET geochemical signatures, which is not a case for the microspherules studied.

Combining these models with chemical and mineralogical features of the microspherules studied, we suggest that the hollow magnetic microspherules from the BWD-1 site are plausibly a result of the ablation of a meteorite(s) during its passage through the Earth's atmosphere at altitudes below 25 km, including the possibility of surface impact. However, until direct evidence of the presence of the meteoritic component in the LYDB sediments is found (e.g. elevated concentrations of the PGE, the presence of the PGE-rich microspherules and magnetite spherules containing wüstite), there is no unequivocal support for the cosmic origin of the hollow magnetic microspherules from the BWD-1 site.

The presence of a high number of the hollow magnetic microspherules can be used for identification of the LYDB. Although some scientists failed to find any microspherules at all along the LYDB in the BWD-1 site (Surovell *et al.* 2009), others reported strongly elevated concentrations of the magnetic microspherules here (Firestone *et al.* 2007; LeCompte *et al.* 2012). Our observations confirm those made by Firestone *et al.* (2007) and LeCompte *et al.* (2012). In spite of the failure to find microspherules along the LYDB, Surovell *et al.* (2009) reported a number of magnetic microspherules in sediments located above the LYDB (not as a discrete microspherule-rich layer though). Such a distribution of the microspherules can be explained by redeposition in younger sediments of the microspherules delivered from along the LYDB. It is appropriate to suggest that Surovell *et al.* (2009) just failed to sample the microspherule-rich layer because it is visually featureless in the BWD-1 site and is very difficult to identify in the field. Overall, in order to use the magnetic microspherules as a stratigraphic marker, it would be necessary to conduct thorough sampling of the sediments in the region of the suggested LYDB location.

Conclusions

Strongly elevated concentrations of the magnetic microspherules in a thin sandy layer corresponding to the LYDB are revealed for the BWD-1 sedimentary sequence. Sharp increase of the number of microspherules in sediments located along the LYDB is in agreement with observations made by Firestone *et al.* (2007, 2010) and LeCompte *et al.* (2012). Because overall close chemical, mineralogical, and structural similarity of the BWD-1 hollow microspherules to those directly related to known meteorite occurrences and/or meteoritic events, the cosmic origin of the former seems to be a credible hypothesis. If we accept such origin of the BWD-1 microspherules, then ablation of iron or stony meteorites during their passage through the Earth's atmosphere seems to be the most plausible mechanism for their formation. However, the exact mechanism of the formation of the magnetic microspherules is not completely clear. In addition to the formation during ablation of the meteoritic body in the Earth's atmosphere (as in the case of the microspherules studied), they could be produced during the airburst of such a body, or could result from the impact of the ET body. When meteorite influx increases, it results, in particular, in elevated concentration of the hollow magnetic microspherules in discrete layers of terrestrial sediments. The elevated concentration of microspherules of the BWD-1 type is a known phenomenon for multiple LYDB locales across North America (e.g. Firestone *et al.* 2007; LeCompte *et al.* 2012; Pigati *et al.* 2012; Wittke *et al.* 2013). The presence of the high number of such microspherules in the sediments can serve as a local stratigraphic marker in identification of the LYDB there where dark variety of the black mat is absent. If one applies methods of microstratigraphy to paleosols of the suggested (LYDB) age, the strongly elevated concentrations of magnetic microspherules would mark precisely the time of around 12.9 ka BP. The data from the present study along with observations made on sediments around the LYDB elsewhere suggest that some unusual event took place just before the onset of the YD climate oscillation. However, an understanding of what happened at *c.* 12.9 ka BP and how it is related (if at all) to the onset of the YD climate oscillation requires further search.

Acknowledgements

The authors are extremely grateful to C.V. Haynes for his invaluable help through the whole duration of their work on the present project. They thank E. Buchner, C. Guaita, M. Maurette and M.S. Sisodia for very fruitful discussions on the subject of the origin of the microspherules. The authors are very grateful to W. Mahaney and an anonymous reviewer for critical reading of the earlier version of the manuscript and for invaluable comments. They thank K. Dominik who helped with the microprobe analyses, and R. Downs and H. Yang for help with the XRD analyses and interpretation of the results.

Alexandre V. Andronikov, Barbara Lafuente, Department of Geosciences, University of Arizona, 1040 E. 4th Street, Tucson, AZ 85721, USA
Email: alexandronikov@gmail.com, barbaralafuente @email.arizona.edu

Irina E. Andronikova, Dante S. Lauretta, Lunar and Planetary Laboratory, University of Arizona, 1415 N. 6th Ave., Tucson, AZ 85705, USA
Email: irandron@yahoo.com, lauretta@orex.lpl.arizona.edu

Clayton W. Loehn, Shared Instrumentation Facility, Institute for Advanced Materials, Baton Rouge, LA 70803, USA
Email: cloehn@lsu.edu

Jesse A.M. Ballenger, Statistical Research Inc., 6099 East Speedway Blvd., Tucson, AZ 85751, USA
Email: jamb@email.arizona.edu

George T. Crawford, Eastern New Mexico University, 1500 South Ave. K, Portales, NM 88130, USA
Email: george.crawford@enmu.edu

References

Anders, E. and Grevesse, N., 1989. Abundances of the elements: meteoritic and solar. *Geochimica et Cosmochimica Acta*, 53, 197–214.

Andronikov, A.V., Lauretta, D.S., Andronikova, I.E. and Maxwell, R.J., 2011. On the possibility of a Late Pleistocene extraterrestrial impact: LA-ICP-MS analysis of the black mat and Usselo horizon samples. *Meteoritics and Planetary Science*, 46(S1), A11.

Andronikov, A.V., Subetto, D.A., Lauretta, D.S., Andronikova, I.E., Drosenko, D.A., Kuznetsov, D.D., Sapelko, T.V. and Syrykh, L.V., 2014. In search for fingerprints of an extraterrestrial event: Trace element characteristics of sediments from the lake Medvedevskoye (Karelian Isthmus, Russia). *Doklady Earth Sciences*, 457, 818–822.

Badyukov, D.D. and Raitala, J., 2012. Ablation spherules in the Sikhote Alin meteorite and their genesis. *Petrology*, 20, 574–582.

Ballenger, J.S.M., Holliday, V.T., Kowler, A.L., Reitze, W.T., Prasciunas, M.M., Miller, D.S. and Windingstad, J.D., 2011. Evidence for Younger Dryas global climate oscillation and human response in the American Southwest. *Quaternary International*, 242, 502–519.

Berger, W.H., 1990. The Younger Dryas cold spell – a quest for causes. *Global and Planetary Change*, 3, 219–237.

Bi, D., Morton, R.D. and Wang, K., 1993. Cosmic nickel-iron alloy spherules from Pleistocene sediments of Alberta, Canada. *Geochimica et Cosmochimica Acta*, 57, 4129–4136.

Bignami, L., Guaita, C., Pezzotta, F. and Zilioli, M., 2014. Micro-spherules near the Kamil crater. *Memorie della Societá Astronomica Italiana Supplementi*, 26, 25–37.

Björck, S., 2007. Younger Dryas oscillation, global evidence. In: Scott, A.E. (ed.), *Encyclopedia of Quaternary Science*. Oxford, Elsevier. 1983–1995.

Blanchard, M.B., 1972. Artificial meteorite ablation studies: iron oxides. *Journal of Geophysical Research*, 77, 2442–2455.

Blanchard, M.B. and Cunningham, G.G., 1974. Artificial meteor ablation studies: Olivine. *Geophysical Research Letters*, 83, 1793–1808.

Blanchard, M.B. and Davis, A.S., 1978. Analysis of ablation debris from natural and artificial iron meteorites. *Journal of Geophysical Research*, 83, 1793–1808.

Blanchard, M.B., Brownlee, D.E., Bunch, T.E., Hodge, P.W. and Kyte, F.T., 1980. Meteoroid ablation spheres from deep-sea sediments. *Earth and Planetary Science Letters*, 46, 178–190.

Bonté, Ph., Jéhanno, C., Maurette, M. and Brownlee, D.E., 1987. Platinum metals and microstructure in magnetic deep sea cosmic spherules. *Journal of Geophysical Research*, 92, E641–E648.

Brauer, A., Haug, G.H., Dulski, P., Sigman, D.M. and Negendank, J.F.W., 2008. An abrupt wind shift in Western Europe at the onset of the Younger Dryas cold period. *Nature Geoscience*, 1, 520–523.

Brownlee, D.E., Bates, B.A. and Wheelock, M.M., 1984. Extraterrestrial platinum group nuggets in deep-sea sediments. *Nature*, 309, 693–695.

Brownlee, D.E., Blanchard, M.B., Cunningham, G.C., Beauchamp, R.H. and Fruland, R., 1975. Criteria for identification of ablation debris from primitive meteoritic bodies. *Journal of Geophysical Research*, 80, 4917–4924.

Bunch, T.E., Hermes, R.E., Moore, A.M.T., Kennett, D.J., Weaver, J.C., Wittke, J.H., DeCarli, P.S., Bischoff, J.L., Hillman, G.C., Howard, G.A., Kimbel, D.R., Kletetschka, G., Lipo, C.P., Sakai, S., Revay, Z., West, A., Firestone, R.B. and Kennett, J.P., 2012. Very high-temperature impact melt products as evidence for cosmic airbursts and impacts 12,900 years ago. *Proceedings of the National Academy of Sciences USA*, 109, 1903–1912.

Colombetti, A., Ferrari, G., Nicolodi, F. and Panini, F., 1998. Some metallic spherules in calcareous-marly sediments of the Romano Flysch, Sestola-Vidiciatico tectonic unit (Modena district, Northern Apennines, Italy). *Planetary and Space Science*, 46, 329–340.

Cornen, G., Bandet, Y., Giresse, P. and Maley, J., 1992. The nature and chronostratigraphy of Quaternary pyroclastic accumulations from Lake Barombi Mbo (West-Cameroon). *Journal of Volcanology and Geothermal Research*, 51, 357–374.

Cronholm, A. and Schmitz, B., 2010. Extraterrestrial chromite distribution across the mid-Ordovician Puxi River section, central China: evidence for a global major spike in flux of L-chondrite matter. *Icarus*, 208, 36–48.

Del Monte, M., Nanni, T. and Tagliazucca, M., 1974a. Origin of cavities in black magnetic spherules. *Journal of Geophysical Research*, 79, 4375–4378.

Del Monte, M., Nanni T. and Tagliazucca, M., 1974b. Ferromagnetic volcanic particulate matter and black magnetic spherules: a comparative study. *Journal of Geophysical Research*, 80, 1880–1884.

Del Monte, M., Nanni, T. and Tagliazucca, M., 1976. The origin of black magnetic spherules through a study of their chemical, physical and mineralogical characteristics. *Annals of Geophysics*, 29, 9–25.

Dredge, I., Parnel, J., Lindgren, P. and Bowden, S., 2010. Elevated flux of cosmic spherules (micrometeorites) in Ordovician rocks of the Durness Group, NW Scotland. *Scottish Journal of Geology*, 46, 7–16.

El Goresey, A., 1968. Electron microprobe analysis and ore microscopic study of magnetic spherules and grains collected from the Greenland ice. *Contributions to Mineralogy and Petrology*, 17, 331–346.

El Goresey, A. and Fechtig, H., 1967. Fusion crust of iron meteorites and mesosiderites and production of cosmic spherules. *Smithsonian Contributions to Astrophysics*, 11, 391–397.

Evans, G.L., 1951. Prehistoric wells in Eastern New Mexico. *American Antiquity*, 17, 1–9.

Fayek, M., Anovitz, L.M., Allard, L.F. and Hull, S., 2012. Framboidal iron oxide: chondrite-like material from the black mat, Murray Springs, Arizona. *Earth and Planetary Science Letters*, 319–320, 251–258.

Firestone, R.B., West, A., Kennett, J.P., Bunch, T.E., Revay, Z.S., Schultz, P.H., Belgya, T., Kennett, D.J., Erlandson, J.M., Dickenson, O.J., Goodyear, A.C., Harris, R.S., Howard, G.A., Kloosterman, J.B., Lechler, P., Mayewski, P.A., Montgomery, J., Poreda, R., Darrah, T., Que Hee, S.S., Smith, A.R., Stich, A., Topping, W., Wittke, J.H. and Wolbach, W.S., 2007. Evidence for an extraterrestrial impact 12,900 years ago that contributed to the megafaunal extinctions at the Younger Dryas cooling. *Proceedings of the National Academy of Sciences USA*, 104, 16016–16021.

Firestone, R.B., West, A., Revay, Z., Hagstrumd, J.T., Belgya, T., Que Hee, S.S. and Smith, A.R., 2010. Analysis of the Younger Dryas Impact Layer. *Journal of Siberian Federal University. Engineering and Technologies*, 1, 30–62.

Franzén, L.G., 2006. Mineral matter, major elements and trace elements in raised bog peat: a case study from southern Sweden, Ireland and Tierra del Fuego, south Argentina. In: Martini, I.P., Martinez Cortizars, A. and Chesworth, W. (eds.), Elsevier B.V., Amsterdam. 241–269.

Franzén, L.G. and Cropp, R.A., 2007. The Peatland/Ice Age hypothesis revised, adding a possible glacial pulse trigger. *Geografiska Annaler*, 84, 301–330.

Fraundorf, P., Lyons, T. and Schubert, P., 1982. The survival of solar flack tracks in interplanetary dust silicates on deceleration in the Earth's atmosphere. *Journal of Geophysical Research*, 87, A409–A417.

Gál-Sólymos, K. and Don, G., 2004. New results on magnetic spherules from Hungary. *Acta Geologica Hungarica*, 47, 287–296.

Genge, M.J., Engrand, C., Gounelle, M. and Taylor, S., 2008. The classification of micrometeorites. *Meteoritics & Planetary Science*, 43, 497–515.

Grachev, A.F., Korchagin, O.A., Tselmovich, V.A. and Kollmann, H.A. 2008. Cosmic dust and micrometeorites in the transitional clay layer at the Cretaceous–Paleogene boundary in the Gams Section (Eastern Alps): morphology and chemical composition. *Izvestya, Physics of the Solid Earth*, 44, 555–569.

Grebennikov, A.V., 2011. Silica-metal spherules in ign-imbrites of Southern Primorye, Russia. *Journal of Earth Science*, 22, 20–31.

Greshake, A., Klöck, W., Arndt, P., Maetz, M., Flynn, G.J., Bajt, S. and Bischoff, A., 1998. Heating experiments simulating atmospheric entry heating of micrometeorites. Clues to their parent body sources. *Meteoritics & Planetary Science*, 33, 267–290.

Guaita, C. and Martegani, F., 2008. Cosmic Microsphere: a SEM study. *Memorie della Societá Astronomica Italiana Supplementi*, 12, 110–125.

Haynes, C.V. Jr, 1995. Geochronology of paleoenvironmental change, Clovis type site, Blackwater Draw, New Mexico. *Geoarchaeology*, 10, 317–388.

Haynes, C.V., 2007. Nature and origin of the black mat, Stratum F_2. In: Haynes, C.V. and Huckell, B.B. (eds), *Murray Springs. A Clovis Site with Multiple Activity Areas in the San Pedro Valley, Arizona*. Anthropological papers of the University of Aricona 71, 240–249.

Haynes, C.V., 2008. Younger Dryas "black mat" and the Rancholabrean termination in North America. *Proceedings of the National Academy of Sciences USA*, 105, 6520–6525.

Haynes, C.V. Jr, Boerner, J., Domanik, K., Lauretta, D., Ballenger, J. and Goreva, J., 2010. The Murray Spring Clovis site, Pleistocene extinction, and the question of extraterrestrial impact. *Proceedings of the National Academy of Sciences USA*, 107, 4010–4015.

Hester, J., 1972. Blackwater Locality No. 1: A Stratified Early Man Site in Eastern New Mexico. *In: Publication of the Fort Burgwin Research Center*, 89, 22–238, Dallas.

Holliday, V.T., 1985. New data on the stratigraphy and pedology of the Clovis and Plainview sites, Southern High Plains. *Quaternary Research*, 23, 388–402.

Holliday, V.T., 1997. *Paleoindian Geoarchaeology of the Southern High Plains*. Texas Archaeology and Ethnohistory Series (Hester, T.R. ed.). University of Texas Press, Austin, TX, 299 p.

Horng, C.-S., Huh, C.-A., Chen, K.-H., Huang, P.-R., Hsiung, K.-H. and Lin, H.-L., 2009. Air pollution history elucidated from anthropogenic spherules and their magnetic signatures in marine sediments offshore of Southwestern Taiwan. *Journal of Marine Systems*, 76, 468–478.

Israde-Alcántara, I., Bischoff, J.L., Domíniguez-Vásquez, G., Li, H.-C., DeCarli, P.S., Bunch, T.E., Wittke, J.H., Weaver, J.C., Firestone, R.B., West, A., Kennett, J.P., Mercer, C., Xie, S., Richman, E.K., Kinzie, C.R. and Wolbach, W.S., 2012. Evidence from central Mexico supporting the Younger Dryas extraterrestrial impact hypothesis. *Proceedings of the National Academy of Sciences USA*, 109, E738–E747.

Iwahashi, J., 1991. Shape and surface structure of the magnetic micro-spherules from Permian and Triassic bedded chert. *Journal of Geosciences*, 34, 55–73.

Jochum, K.P., Weis, U., Stoll, B., Kuzmin, D., Yang, Q., Raczek, I., Jacob, D.E., Stracke, A., Birbaum, K., Frick, D.A., Günther, D. and Enzweiler, J., 2011. Determination of reference values for NIST SRM 610–617 glasses following ISO Guidelines. *Geostandards and Geoanalytical Research*, 35, 397–429.

Katz, L., 1997. *The History of Blackwater Draw*. Eastern New Mexico University Printing Services, Portales, NM, 25 p.

Kennett, D.J., Kennett, J.P., West, A., West, G.J., Bunch, T.E., Culleton, B.J., Erlandson, J.M., Que Hee, S.S., Johnson, J.R., Mercer, C., Shen, F., Seller, M., Stafford, T.W., Stich, A., Weaver, J.C., Wittke, J.H. and Wolbach, W.S., 2009. Shock-synthesized hexagonal diamonds in

Younger Dryas boundary sediments. *Proceedings of the National Academy of Sciences USA*, 106, 12623–12628.

Kennett, J.P., Kennett, D.J., Culleton, B.J., Tortosa, J.E.A., Bischoff, J.L., Bunch, T.E., Daniel, I.R. Jr, Erlandson, J.M., Ferraro, D., Firestone, R.B., Goodyear, A.C., Israde-Alcantara, I., Johnson, J.R., Jorda Pardo, J.F., Kimbel, D.R., LeCompte, M.A., Lopinot, N.H., Mahaney, W.C., Moore, A.M.T., Ray, J.H., Stafford., T.W. Jr, Tankersley, K.B., Wittke, J.H., Wolbach, W.S. and West, A., 2015. Bayesian chronologic analyses consistent with synchronous age of 12,835–12,735 Cal B.P. for Younger Dryas boundary on four continents. *Proceedings of the National Academy of Sciences USA*, 112, E4344–E4353.

Kim, B.Y., Kodama, K.P. and Moeller, R.E., 2005. Bacterial magnetite produced in water column dominates lake sediment mineral magnetism: Lake Ely, USA. *Geophysical Journal International*, 163, 26–37.

Koeberl, C. and Hagen, G., 1989. Extraterrestrial spherules in glacial sediments from the Transantarctic Mountains, Antarctica: structure, mineralogy, and chemical composition. *Geochimica et Cosmochimica Acta*, 53, 937–944.

Kopp, R.E., Weiss, B.P., Maloof, A.C., Vali, H., Nash, C.Z. and Kirschvink, J.L., 2006. Chains clumps and strings: magnetofossil taphonomy with ferromagnetic resonance spectroscopy. *Earth and Planetary Science Letters*, 247, 10–25.

LeCompte, M.A., Goodyear, A.C., Demitroff, M.N., Batchelor, D., Vogel, E.K., Mooney, C., Rock, B.N. and Seidel, A.W., 2012. Independent evaluation of conflicting microspherule results from different investigations of the Younger Dryas impact hypothesis. *Proceedings of the National Academy of Sciences USA*, 109, E2960–E2969.

Lindskog, A., Schmitz, B., Cronholm, A. and Dronov, A., 2012. A Russian record of a Middle Ordovician meteorite shower: extraterrestrial chromite at Lynna River, St. Petersburg region. *Meteoritics & Planetary Science*, 47, 1274–1290.

Lippert, P.C. and Zachos, J.C., 2007. A biogenic origin for anomalous fine-grained magnetic material at the Paleocene-Eocene boundary at Wilson Lake, New Jersey. *Paleoceanography*, 22, 1–8.

Lowe, J.J., Rasmussen, S.O., Björck, S., Hoek, W.Z., Steffensen, J.P., Walker, M.J.C., Yu, Z.C. and INTIMATE group, 2008. Synchronisation of palaeoenvironmental events in the North Atlantic region during the Last Termination: a revised protocol recommended by the INTIMATE group. *Quaternary Science Reviews*, 27, 6–17.

Mahaney, W.C., Kalm, V., Krinsley, D.H., Tricart, P., Schwartz, S., Dohm, J., Kim, K.J., Kapran, B., Milner, M.W., Beukens, R., Boccia, S., Hancock, R.G.V., Hart, K.M. and Kelleher, B., 2010. Evidence from the northwestern Venezuelan Andes for extraterrestrial impact: the black mat enigma. *Geomorphology*, 116, 48–57.

Mahaney, W.C., Keiser, L., Krinsley, D., Kalm, V., Beukens, R. and West, A., 2013. New evidence from a black mat site in the Northern Andes supporting a cosmic impact 12,800 years ago. *Journal of Geology*, 121, 309–325.

Marini, F. and Raukas, A., 2009. Lechatelierite-bearing microspherules from semicoke hill (Kiviõli, Estonia): contribution to contamination problem of natural microtectites. *Oil Shale*, 26, 415–423.

Marini, F., Raukas, A. and Tiirmaa, R., 2004. Magnetic fines from the Kaali impact-site (Holocene, Estonia): preliminary SEM investigation. *Geochemical Journal*, 38, 107–120.

McCabe, C., Sassen, R. and Saffer, B., 1987. Occurrence of secondary magnetite within biodegraded oil. *Geology*, 15, 7–10.

McManus, J.F., Francois, R., Gherardi, J.-M., Keigwin, L.D. and Brown-Legar, S., 2004. Collapse and rapid resumption of Atlantic meridianal circulation linked to deglacial climate changes. *Nature*, 428, 834–837.

McWhinnie, T.S., van der Pluijm, B.A. and van der Voo, R., 1990. Remagnetization and thrusting in the Idaho-Wyoming Overthrust Belt. *Journal of Geophysical Research*, 95, 4551–4559.

Misawa, K., Kohno, M., Tomiyama, T., Noguchi, T., Nakamura, T., Nagao, K., Mikouchi, T. and Nishiizumu, K., 2010. Two extraterrestrial dust horizons found in the Dome Fuji ice core, East Antarctica. *Earth and Planetary Science Letters*, 289, 287–297.

Ohtani, E. and Ringwood, A.E., 1984. Composition of the core, I. Solubility of oxygen in molten iron at high temperatures. *Earth and Planetary Science Letters*, 71, 85–93.

Palme, H., 2008. Platinum-group elements in cosmochemistry. *Elements*, 4, 233–238.

Petaev, M.I., Huang, S., Jacobsen, S.B. and Zindler, A., 2013. Large Pt anomaly in the Greenland ice core points to a cataclysm at the onset of Younger Dryas. *Proceedings of the National Academy of Sciences USA*, 110, 12917–12920.

Peteet, D., 1995. Global Younger Dryas? *Quaternary International*, 28, 93–104.

Pigati, J.S., Bright, J.E., Shanahan, T.M. and Mahan, S.M., 2009. Late Pleistocene paleohydrology near the boundary of the Sonoran and Chihuahuan Desert, southeastern Arizona, USA. *Quaternary Science Reviews*, 28, 286–230.

Pigati, J.S., Latorre, C., Rech, J.A., Betancourt, J.L., Martinez, K.E. and Buddahn, J.R., 2012. Accumulation of impact markers in desert wetlands and implication for the Younger Dryas impact hypothesis. *Proceedings of the National Academy of Science USA*, 109, 7208–7212.

Rochette, P., Folco, L., d'Orazio, M., Suavet, C. and Gattaccecca, J., 2009. Large iron spherules from the Transantarctic Mountains: where is the Nickel? *Meteoritics and Planetary Science*, 44(S7), A176.

Rudraswami, R.G., Shyam, Prasad, M., Babu, E.V.S.S.K., Vijaya Kumar, T., Feng, W. and Plane, J.M.C., 2012. Fractionation and fragmentation of glass cosmic spherules during atmospheric entry. *Geochimica et Cosmochimica Acta*, 99, 110–127.

Rudraswami, R.G., Shyam Prasad, M., Plane, J.M.C., Berg, T., Feng, W. and Balgar, S., 2014a. Refractory metal nuggets in different types of cosmic spherules. *Geochimica et Cosmochimica Acta*, 131, 247–266.

Rudraswami, R.G., Shyam Prasad, M. and Vijaya Kumar, T., 2014b. Chemistry and petrology of Fe-Ni beads from different types of cosmic spherules: Implication

for precursors. *Geochimica et Cosmochimica Acta*, 145, 139–158.

Saffer, B. and McCabe, C., 1992. Further studies of carbonate remagnetization in Northern Appalachian Basin. *Journal of Geophysical Research*, 97, 4331–4348.

Sandford, S.A. and Bradley, J.P., 1989. Interplanetary dust particles collected in the stratosphere: Observations of atmospheric heating and constraints on their interrelationships and sources. *Icarus*, 82, 146–166.

Sawlowicz, Z., 1993. Iridium and other platinum-group elements as geochemical markers in sedimentary environments. *Palaeogeography, Palaeoclimatology, Palaeoecology*, 104, 253–270.

Schmitz, B., Harper, D.A.T., Peucker-Ehrenbrink, B., Stouge, S., Alwmark, C., Cronholm, A., Bergström, S.M., Tassinari, M. and Xiaofeng, W., 2008. Asteroid breakup linked to the Great Ordovician Biodiversification Event. *Nature Geoscience*, 1, 49–53.

Schumann, D., Raub, T.D., Kopp, R.E., Guerquin-Kern, J.-L., Wu, T.-D., Rouiller, I., Smirnov, A.V., Sears, S.K., Lücken, U., Tikoo, S.M., Hesse, R., Kirschvink, J.L. and Vali, H., 2008. Gigantism in unique biogenic magnetite at the Paleocene-Eocene Thermal Maximum. *Proceedings of the National Academy of Sciences USA*, 105, 17648–17653.

Sellards, E.H., 1952. *Early Man in America. A Study in Prehistory.* University of Texas Press, Austin, TX, 211 p.

Stankowski, W.T.J., Katrusiak, A. and Budzianowski, A., 2006. Crystallographic variety of magnetic spherules from Pleistocene and Holocene sediments in the Northern foreland of Morasko-Meteorite Reserve. *Planetary and Space Science*, 54, 60–70.

Stolz, J.H., Lovley, D.R. and Haggerty, S.E., 1990. Biogenic magnetite and the magnetization of sediments. *Journal of Geophysical Research*, 95, 4355–4361.

Suk, D., van der Voo, R. and Peacor, D.R., 1990. Scanning and transmission electron microscope observations of magnetite and other iron phases in Ordovician carbonates from East Tennessee. *Journal of Geophysical Research*, 95, 12327–12336.

Surovell, T.A., Holliday, V.T., Gingerich, J.A.M., Ketron, C., Haynes, C.V. Jr, Hilman, I., Wagner, D.P., Johnson, E. and Claeys, P., 2009. An independent evaluation of the Younger Dryas extraterrestrial impact hypothesis. *Proceedings of the National Academy of Sciences USA*, 109, 18155–18158.

Szöör, Gy., Elekes, Z., Rózsa, P., Uzonyi, I., Simulák, J. and Kiss, Á.Z., 2001. Magnetic spherules: cosmic dust or markers of meteoritic impact? *Nuclear Instruments and Methods in Physic Research Part B*, 181, 557–562.

Teller, J.T., Leverington, D.W. and Mann, J.D., 2002. Freshwater outbursts to the ocean from glacial Lake Agassiz and their role in climate change during the last deglaciation. *Quaternary Science Reviews*, 21, 879–887.

Toppani, A., Libourel, G., Engrand, C. and Maurette, M., 2001. Experimental simulation of atmospheric entry of micrometeorites. *Meteoritics & Planetary Science*, 36, 1377–1396.

Towe, K.M. and Moench, T.T., 1981. Electron-optical characterization of bacterial magnetite. *Earth and Planetary Science Letters*, 52, 213–220.

Tselmovich, V.A., 2013. Space microspherules on the surface of the Chelyabinsk meteorite. *Proceedings of the International Conferences "Asteroids and Comets. A Chelyabinsk Event and Study of the Fall of the Meteorite to the Lake of Chebarkul"*, Kray Ra Press, Chelyabinsk. 140–147. (in Russian)

Tselmovich, V.A., Gindilis, L.M. and Shevelev, G.N., 2013. Analysis of the magnetic fraction in a dust component of the Chelyabinsk meteorite. *Proceedings of the International Conferences "Asteroids and Comets. A Chelyabinsk Event and Study of the Fall of the Meteorite to the Lake of Chebarkul"*, Kray Ra Press, Chelyabinsk. 301–307. (in Russian)

Uscinowicz, G., 2009. Micro-scale magnetic grains from shallow water sediments of the Gulf of Gdansk. *Oceanological and Hydrobiological Studies*, 38, 21–30.

Vali, H., Förster, O., Amarantidis, G. and Petersen, N., 1987. Magnetotactic bacteria and their magnetofossils in sediments. *Earth and Planetary Science Letters*, 86, 389–400.

Van Ginneken, M., Folco, L., Perchiazzi, N., Rochette, P. and Bland, P.A., 2010. Meteoritic ablation debris from the Transantarctic Mountains: Evidence for a Tunguska-like impact over Antarctica ca. 480 ka ago. *Earth and Planetary Science Letters*, 293, 104–113.

Voldman, G.G., Genge, M.J., Albanesi, G.L., Barnes, C.R. and Ortega, G., 2012. Cosmic spherules from the Ordovician of Argentina. *Geological Journal*, 48, 222–235.

Vondrak, T., Plane, J.C.M., Broadley, S. and Janches, D., 2008. A chemical model of meteoritic ablation. *Atmospheric Chemistry and Physics*, 8, 7015–7031.

Vuorelainen, Y. and Törnroos, R., 1986. Man-made Pt-$PtAs_2$ spherules after sperrylite from alluvial deposits in Finnish Lapland. *Canadian Mineralogist*, 24, 523–528.

Wedepohl, K.H., 1995. The composition of the continental crust. *Geochimica et Cosmochimica Acta*, 59, 1217–1232.

Wittke, J.H., Weaver, J.C., Bunch, T.E., Kennett, J.P., Kennett, D.J., Moore, A.M.T., Hillman, G.C., Tankersley, K.B., Goodyear, A.C., Moore, C.R., Daniel, R. Jr, Ray, J.H., Lopinot, N.H., Ferraro, D., Israde-Alcántara, I., Bischoff, J.L., DeCarli, P.S., Hermes, R.E., Kloosterman, J.B., Revay, Z., Howard, G.A., Kimbel, D.R., Kletetschka, G., Nabelek, L., Lipo, C.P., Sakai, S., West, A. and Firestone, R.B., 2013. Evidence for deposition of 10 million tonnes of impact spherules across four continents 12,800 y ago. *Proceedings of the National Academy of Science*, 110, E2088–E2097.

Wu, Y., Sharma, M., LeCompte, M.A., Demitroff, M.N. and Landis, J.D., 2013. Origin and provenance of spherules and magnetic grains at the Younger Dryas boundary. *Proceedings of the National Academy of Sciences USA*, 110, E3557–E3566.

Manuscript received 24 Aug., 2015; revised and accepted 25 Nov., 2015

